Effect of the wavy tank wall on the characteristics of mechanical agitation in the presence of a Al2O3-water nanofluid

Abderrahim Mokhefi, Mohamed Bouanini, Mohammed Elmir, Pierre Spiteri

Metallurgical and Materials Engineering *Research paper*
Association of Metallurgical Engineers of Serbia AMES *https://doi.org/10.30544/626*

EFFECT OF THE WAVY TANK WALL ON THE CHARACTERISTICS OF MECHANICAL AGITATION IN THE PRESENCE OF AN Al_2O_3-WATER NANOFLUID

Abderrahim Mokhefi [1,], Mohamed Bouanini[2], Mohammed Elmir[1], Pierre Spitéri [3]*

[1]Mechanics, Modeling and Experimentation Laboratory L2ME, Faculty of Sciences and Technology, Bechar University B.P.417, 08000, Bechar, Algeria
[2] Structural Mechanics Laboratory L.M.S, Faculty of Sciences and Technology, Bechar University B.P.417, 08000, Bechar, Algeria
[3] INP-ENSEEIHT, IRIT, 2 rue Charles Camichel- BP 7122- 31071 Toulouse CEDEX 7, France

Received 17.03.2021
Accepted 21.04.2021

Abstract

The enhancement of the heat transfer in the stirred tank is a much-desired objective for accelerating certain physical and chemical parameters in the industrial field. From this basis, an attempt is made in this paper to investigate the effect of the wavy wall of a stirred tank on the hydrodynamic, thermal, and energetic behavior of an Al_2O_3-Water nanofluid. The stirred tank has a flat bottom, and it is equipped with an anchor stirrer. A hot temperature has been imposed on the tank wall, and the agitator has been assumed adiabatic, where the nanofluid has a cold temperature at the initial instant. The laminar flow was governed by the equations that describe the forced convection, and it was solved by the finite element method. The numerical simulation results showed a considerable acceleration in the heat transfer inside the stirred tank by increasing the amplitude of the wavy wall and increasing the nanoparticle concentration. However, there has been a remarkable increase in the stirring power number. This contribution aims to increase thermal efficiency, especially in the chemical and petrochemical fields, to obtain a better yield of certain chemical reactions and mass transfer depending on the heat.

Keywords: stirred tank; wavy wall; heat transfer; power number; anchor stirrer; nanofluid.

[*]Corresponding author: Abderrahim Mokhefi, *abderahimmokhefi@yahoo.fr*

Introduction

Many chemical and biochemical industries are carried out in stirred tanks or reactors. The operation of mechanical agitation amplifies the phenomenon of mass and heat transfer in order to provide a certain homogeneity degree of the physical or chemical properties of the product used. Often the performance of these processes is accompanied by the addition or removal of heat.

Most of the work carried out by researchers in the field of mechanical agitation in recent years has focused on one direction, which is the hydrodynamic study of the flow and energy consumption inside agitated tanks in trying to improve them by making geometric modifications to the rotating mobiles on the one hand and to the tanks on the other hand. Many researchers have considered different rheologies of complex fluids and tried to adapt them to specific and suitable equipment geometries.

Rodaina Metaweaet al. [1] have reported a novel design of a batch agitated vessel used for the production of biodiesel from palm oil. They observed a reduction in carbon monoxide and a marginal increase in nitrogen oxide emissions. *Ameur* [2] presented an attempt to reduce the power requirements of Scaba 6SRGT impellers for stirring viscoplastic fluids in a cylindrical unbaffled tank. The perforation diameter, perforation shape, and the number of perforations on the hydrodynamics induced and power consumption have been investigated. He showed that the circular shape had allowed the optimal reduction. *Foukrach et al*. [3] studied the effect of agitator types on the turbulent flows in stirred tanks without and with baffles. They found that the agitator DTBT gives a good reduction of the vortex size of the impeller angles. *Kamla et al*. [4] investigate the effects of the anchor geometry, the number of blades, and their inclination inside a stirred tank for low Reynolds numbers varying from 0.1 to 60. They demonstrate that the lowest power consumption is achieved with the circular shape of blades. *Major‐Godlewska1et al*. [5] have presented the power characteristics for an agitated vessel equipped with short planar baffles and a pitched blade turbine. They showed that the power number function increases with the increase in the angle of the inclination of the impeller blade. *Woziwodzki et al*. [6] studied the efficiency of mixing pseudoplastic fluids using aqueous solutions of the sodium salt of carboxymethylcellulose of varying mass concentrations.

Many other recent numerical works with respect to the stirring process were studied. Among these works, we find *Ameur* [7-9], *Keras et al*. [10], *Amir Heidari* [11].

There is no doubt that the phenomenon of heat transfer inside stirred vessels is one of the important processes which necessarily contributes to improving the quality of the mixture and accelerating the chemical reactions that take place there. Thus, the enhancement of this process is included in the list of works, which have experienced great popularity in recent years, in particular with the occupation of nanofluids [12-17] an important space in various fields of scientific research. As soon as we review previous work in the field of mechanical agitation, a sort of lack emerges from numerical works devoted to the study of heat transfer. *Bertrand* [18] carried out a set of works by numerical voice on hydrodynamics and heat transfer in agitated tanks provided with different types of agitators for Newtonian and non-Newtonian fluids. He studied the thermal behavior in these stirred tanks. *Baccar et al*. [19] gave a numerical hydrodynamic and thermal investigation of the turbulent flows induced in a cylindrical tank, provided with a six-blade radial turbine. They noted a strong contribution of the turbulent flows to the parietal heat transfer, giving place at the uniformity of the temperature field. *Hami et al*. [20] studied the flow and the heat transfer of water in a stirred tank equipped with an anchor

having inclined blades. They noted an increase in the power number according to the inclination angle with a decrease in the number Nusselt. *Benmoussa et al*. [21] presented an investigation of the inertia effect and the plasticity influence on the thermal and hydrodynamic profile for a stirred system; they found that thermal performance is intimately linked to the hydrodynamic state of the whole of the agitated tank. *Srinivas et al*. [22] studied the performance of a stirred helical coil heat exchanger using an alumina-water nanofluid in terms of energy consumed to heat another fluid. They observed that increasing the agitator rotation speed and the fluid temperature resulted in more energy savings. *Thangavelu et al*. [23] conducted a comparative study on enhancing heat transfer using a nanofluid in a spirally agitated container. They found that the heat transfer coefficient of nanofluid became higher than that of water and increased with the volume fraction. *Marcela Věříšová et al*. [24] In their work, heat transfer via the cylindrical part of the jacket in an agitated vessel has been analyzed. They are summarized in the form of Nusselt number correlations describing their dependency on the Reynolds number. *Korib et al.* [25], in their work, carried out a numerical simulation to study the fluid flow and the heat transfer around a circular cylinder rotating on low Reynolds numbers. Among their findings, the mean Nusselt number decreases with increasing rotational rate, and the suppression of heat transfer due to rotation increases with increasing the rotation speed.

The present study contributes by way of numerical simulation to the hydrodynamic and thermal study of internal laminar flows induced by a mechanically stirred tank anchor. It appears that no work was reported on the effect of the wavy wall on the stirring flow phenomena. Hence, our objective through this study is to highlight the effect of the shape of a laterally wavy tank wall on the hydrodynamic and thermal structures and on the energy consumption of a nanofluid. The study will be carried out by taking the effect of the wavenumber, the wave amplitude, and the concentration of nanoparticles. This makes it possible in particular to explore the degree of efficiency of the corrugated shape of the vessel and of the addition of nanoparticles during mechanical agitation.

Geometric description

The anchor is recognized to be an agitator used to sweep high viscous fluids, create predominant tangential motion as well as improve heat transfer. In the same context, the introduction of the wavy tank walls presents one of the factors, which make it possible to increase the contact surface between the fluid and the hot wall. On the other hand, the addition of nanoparticles helps to increase the thermal conductivity of the liquid. The present stirred tank to have a cylindrical wavy shape of medium diameter (D) and height (H) with a flat bottom. It is filled with Al_2O_3-water nanofluid and equipped with a standard anchor of diameter (d), length (L), thickness (w), and height (h). The shaft of this anchor is of diameter (da). The anchor rotates with a frequency (N). The undulation of the side tank wall follows at each level z the following mathematical formula:

$$\begin{cases} X = (R + a\cos n\theta)\cos\theta \\ Y = (R + a\cos n\theta)\sin\theta \end{cases} \qquad 1$$

With a is the wave amplitude and n is the wave number.

Due to the symmetry of the anchor shape and its symmetrically sweeping fluid at all horizontal levels of the tank, the study was viewed in two dimensions. The geometry

of the configuration with the coordinate system is shown schematically in Figure 2. On this configuration, a constant hot temperature (T_h) has been imposed as a function of time on the wavy tank wall. The nanofluid comprises at an initial instant a cold temperature (T_c) that increases as a function of time towards (T_h). The walls of the stirrer are assumed adiabatic and rotating with a uniform frequency of rotation (N). Radiation, work under pressure, and viscous dissipation is assumed negligible in the heat equation.

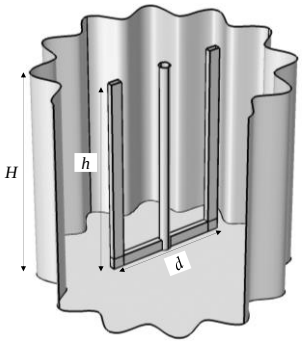

Fig. 1. Stirred wavy tank equipped with an anchor.

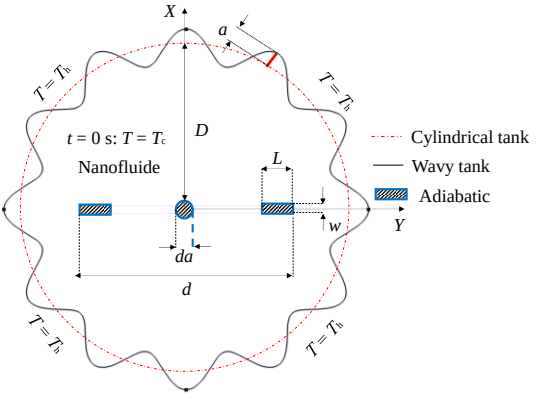

Fig. 2. Cross-section of the stirred wavy tank fitted with the anchor.

The geometric ratios used are: d/D=0.779, da/D=0.025, L/D=0.02 and w/D=0.074. The fluid properties are also assumed to be constant (tab 1.), the gravitational acceleration has been neglected, and the tank wall is assumed non-slip and rigid.

Table 1. Physical properties of base fluid and alumina nanoparticles [26].

Properties	Density [kg/m^3]	Thermal capacity [J/(kg.K)]	Thermal conductivity W.m^{-1}.K^{-1}]	Dynamic viscosity [kg/(m.s)]
Water	998.2	4182	0.597	$9.93.10^{-4}$
Al_2O_3	3880	773	36	/

Mathematical Model

In nanofluid mechanics, the movement of fluids is governed by the laws of conservation of mass, momentum, and energy. The dimensionless continuity equation remains unchanged, but the moment and dimensionless heat equations are modified by introducing the physical properties of the nanofluid according to the laws of suspension.

$$\frac{\partial U^*}{\partial X^*}+\frac{\partial V^*}{\partial Y^*}=0 \qquad 2$$

$$\frac{\partial U^*}{\partial \tau}+U^*\frac{\partial U^*}{\partial X^*}+V^*\frac{\partial U^*}{\partial Y^*}=-\frac{\partial P^*}{\partial X^*}+\frac{2}{\pi}\left(\frac{d}{D}\right)^2\frac{\rho_{\mathrm{f}}}{\rho_{\mathrm{nf}}}\frac{\mu_{\mathrm{nf}}}{\mu_{\mathrm{f}}}\frac{1}{\mathrm{Re}}\left(\frac{\partial^2 U^*}{\partial X^{*2}}+\frac{\partial^2 U^*}{\partial Y^{*2}}\right) \qquad 3$$

$$\frac{\partial V^*}{\partial \tau}+U^*\frac{\partial V^*}{\partial X^*}+V^*\frac{\partial V^*}{\partial Y^*}=-\frac{\partial P^*}{\partial Y^*}+\frac{2}{\pi}\left(\frac{d}{D}\right)^2\frac{\rho_{\mathrm{f}}}{\rho_{\mathrm{nf}}}\frac{\mu_{\mathrm{nf}}}{\mu_{\mathrm{f}}}\frac{1}{\mathrm{Re}}\left(\frac{\partial^2 V^*}{\partial X^{*2}}+\frac{\partial^2 V^*}{\partial Y^{*2}}\right) \qquad 4$$

$$\frac{\partial T^*}{\partial \tau}+U^*\frac{\partial T^*}{\partial X^*}+V^*\frac{\partial T^*}{\partial Y^*}=\frac{2}{\pi}\left(\frac{d}{D}\right)^2\frac{\alpha_{\mathrm{nf}}}{\alpha_{\mathrm{f}}}\frac{1}{\mathrm{Re}\,\mathrm{Pr}}\left(\frac{\partial^2 T^*}{\partial X^{*2}}+\frac{\partial^2 T^*}{\partial Y^{*2}}\right) \qquad 5$$

For writing dimensionless equations, the variables used are:

$$\tau=2\pi Nt,\quad X^*=\frac{2X}{D},\quad Y^*=\frac{2Y}{D},\quad U^*=\frac{U}{\pi ND},\quad V^*=\frac{V}{\pi ND},$$

$$P^*=\frac{P}{\rho(\pi ND)^2}\quad T^*=\frac{T-T_c}{T_h-T_c} \qquad 6$$

The dimensionless numbers appearing in the equations (3-6) are the Reynolds and Prandtl number:

$$\mathrm{Re}=\frac{\rho_{\mathrm{f}}Nd^2}{\mu_{\mathrm{f}}},\quad \mathrm{Pr}=\frac{\mu_{\mathrm{f}}Cp_{\mathrm{f}}}{k_{\mathrm{f}}} \qquad 7$$

The physical properties of the nanofluid: density, dynamic viscosity [27], thermal conductivity [28], and specific heat are respectively calculated by:

$$\rho_{\mathrm{nf}}=\varphi\rho_{\mathrm{p}}+(1-\varphi)\rho_{\mathrm{f}} \qquad 8$$

$$\mu_{nf} = \mu_f (1-\varphi)^{-2.5} \quad (9)$$

$$\frac{k_{nf}}{k_f} = \frac{k_p + 2k_f - 2\varphi(k_f - k_p)}{k_p + 2k_f + \varphi(k_f - k_p)} \quad (10)$$

$$(\rho Cp)_{nf} = \varphi(\rho Cp)_f + (1-\varphi)(\rho Cp)_p \quad (11)$$

Thermal diffusivity is calculated by:

$$\alpha = \frac{k}{\rho Cp} \quad (12)$$

With φ is the volume fraction of the nanoparticles.
The dimensionless tangential and radial velocities are calculated by [18]:

$$V_\theta^* = \frac{-U^*Y^* + V^*X^*}{\sqrt{X^{*2} + Y^{*2}}}, \quad V_r^* = \frac{U^*X^* + V^*X^*}{\sqrt{X^{*2} + Y^{*2}}} \quad (13)$$

The Initial and the boundary conditions can be written by:
At the instant $\tau = 0$

The wall of the tank: U = V* = 0, T* = 1* (14)

The whole tank: T = 0* (15)

The stirrer: V_θ = r/D, Vr* = 0; $\partial_N T$ * = 0* (16)

At the instant $\tau \geq 0$

The wall of the tank: U = V* = 0, T* = 1* (17)

The stirrer: V_θ = r/D, Vr* = 0; $\partial_N T$* = 0* (18)

The power number [29] for the nanofluid is calculated by the formula:

$$\mathrm{Np} = \frac{\mu_{nf}}{\mu_f}\left(\frac{D}{d}\right)^3 \frac{\pi^2}{\mathrm{Re}} \iint_{\text{Tnak volume}} Q_V^* \mathrm{d}X^* \mathrm{d}Y^* \quad (19)$$

The average Nusselt number at the hot wall and at each instant τ is given by:

$$\mathrm{Nu} = \mathrm{Nu}(\tau) = \frac{k_{\mathrm{nf}}}{k_{\mathrm{f}}} \int_{\text{Tank wall}} \frac{\partial T^*}{\partial \mathrm{s}^*} \times r'(\theta)\,\mathrm{d}\theta \qquad 20$$

The dimensionless stream function is defined by:

$$\frac{\partial \Psi^*}{\partial X^*} = -V^* \quad , \quad \frac{\partial \Psi^*}{\partial Y^*} = U^* \qquad 21$$

Numerical method

The system of equations accompanied by the boundary conditions has been solved by the Galerkin finite element formulation. The interpolation functions in terms of local normalized element coordinates have been used to approximate the dependent variables within each element. Details of the method are available in *Taylor and Hood* [30] and *Dechaumphai* [31]. The mesh adopted has a triangular shape and is refined close to the walls of the anchor and the tank because of the geometry complexity of these zones generated by the change in the wavenumber.

To ensure the consistency of our results and to obtain results very close to those existing in the literature, we have tested several meshes. Table 2 shows the number of elements used during the simulation and the change in the values of the power number (Np), tangential velocity, and radial velocity in a point (X* = 0, Y* = 0.5) of the study domain. The mesh test was carried out for the case of a wavy wall tank with n = 6 and A = 0.1; the nanofluid introduced at a concentration φ = 0.04 and at Re = 10. We opted for the mesh corresponding to a number of elements equal to 88390 with regard to the last two values of the power number, the tangential and radial velocities, which are almost identical. Moreover, the computation time is not too prohibitive. The selected convergence criterion relates to the relative error of each dependent variable, which must be less than 10^{-6}.

Table 2. Variation of certain parameters depending on the elements number.

elements	Np	*Vt**	*Vr**
75264	17.019	0.3255	0.0541
88390	17.018	0.3255	0.0541
101514	17.018	0.3254	0.0541

In order to attest to the reliability of the numerical simulation and the conformity of the results, we deemed it necessary to validate our simulations. Indeed, we referred to the work of *Hami et al*. [20] and *Bertrand* [18] using the same simulation conditions to ensure the similarity of the numerical results. We have put forward a global parameter, which is the power number (Figure 3 (b)) for different Reynolds number. On the other hand, we compared the tangential velocity (Figure 3 (a)) for the same references except that for the reference [18], where we compared with experimental results. The comparison of our results with those obtained by [20] and [18] shows a very satisfactory agreement.

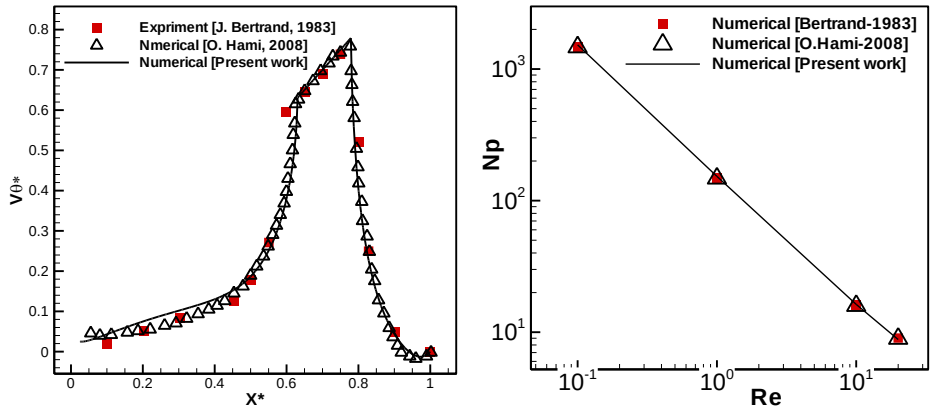

(a) *(b)*

Fig. 3. Comparison of the present data with the references [18] and [20] (a) Tangential velocity(b) Power number.

Results and discussion

It is widely recognized in various fields of scientific research, especially those that study the improvement of heat transfer, that the use of wavy walls has become a common and widely used technique due to their efficiency in increasing the contact surface between fluids and walls subjected to certain temperatures. On the other hand, current scientific research work is challenging without the introduction of nanofluids as alternative supports for conventional fluids, particularly in the field of heat transfer. There is also no doubt that the process of mixing and mechanical stirring hardly leaves a single industrial field because of its remarkable importance and, in particular, in the acceleration of chemical reactions. Based on the importance mentioned, the present study adds a new contribution to this field which aspires to extract the effect of tanks whose wall is wavy with a different number (n = 0 to 30) and different amplitude (A = 0 to 0.1) as well as the inclusion of alumina nanoparticles in water for different concentrations (φ = 0 to 0.1) on the hydrodynamic and thermal behavior inside a tank equipped with an anchor stirrer. Due to the multiplicity of studies wishing to investigate the effect of inertia on the hydrodynamic behavior using anchor agitators, it has been decided in this study to fix the Reynolds and Prandtl number at the values Re = 10 and Pr = 7, which are suitable for the laminar flow regime. The results that will be highlighted here include the effect of the parameters already mentioned on some local characteristics such as velocity field, temperature profile by highlighting: nanofluid streamlines, isotherms, tangential velocity curves, and radial and temperature curves. On the other hand, we will show the changes in the global characteristics, which are represented here by the power number and the Nusselt number.

The wavenumber effects

Concerning the hydrodynamics of nanofluids, in the case of stirred tanks, the addition of waves to the wall can cause local stagnation of the fluid inside the waves, in particular those which are not in the position of the rotating mobile, it can cause a

contraction in the convective transfer and on the other hand the promotion of the heat transfer by conductive mode.

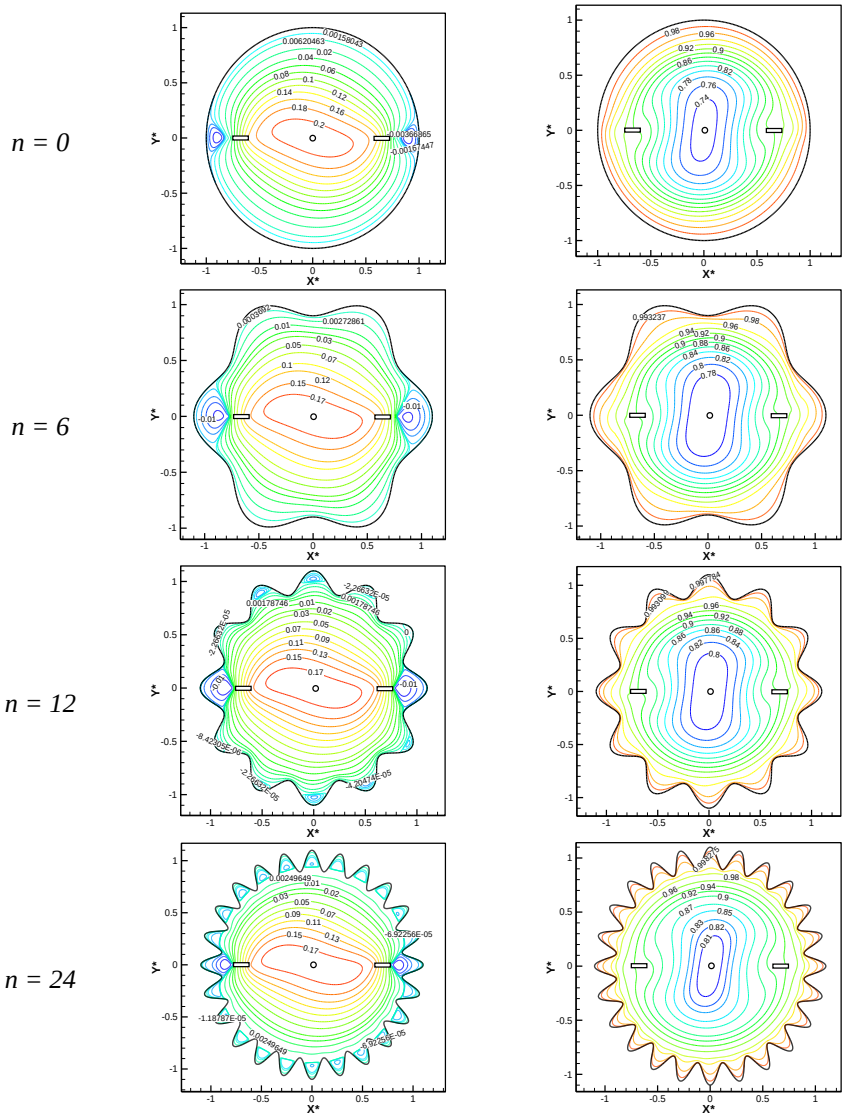

Fig. 4. Streamlines (left column) and isotherms (right column) for different wavenumbers with A = 0.1 and φ = 0.04 at τ = 44.

Figure 4 illustrates the streamlines and isotherms for different wavenumber $n = 0$ (standard case), 6, 12, and 24. The concentration of nanoparticles and the amplitude of the wave were respectively set at 0.04 and 0.1. By comparing the shape of the streamlines and the isotherms for the case of a non-wavy tank and a wavy tank, we see that the presence of the waves causes a notable decrease in the maximum stream function from

0.2 to 0.17 for n = 24. On the other hand, a remarkable temperature rise was observed at the instant τ = 44, due to the contraction of the isothermal lines towards the shaft with the rise in the wavenumber.

The examination of the streamlines shape with an increase in the number of waves allows us to observe the formation of a recirculation region of the nanofluid within the two waves adjacent to the anchor, while we notice the formation of nanofluid stagnation regions within all waves in the case of n = 12 and 24.

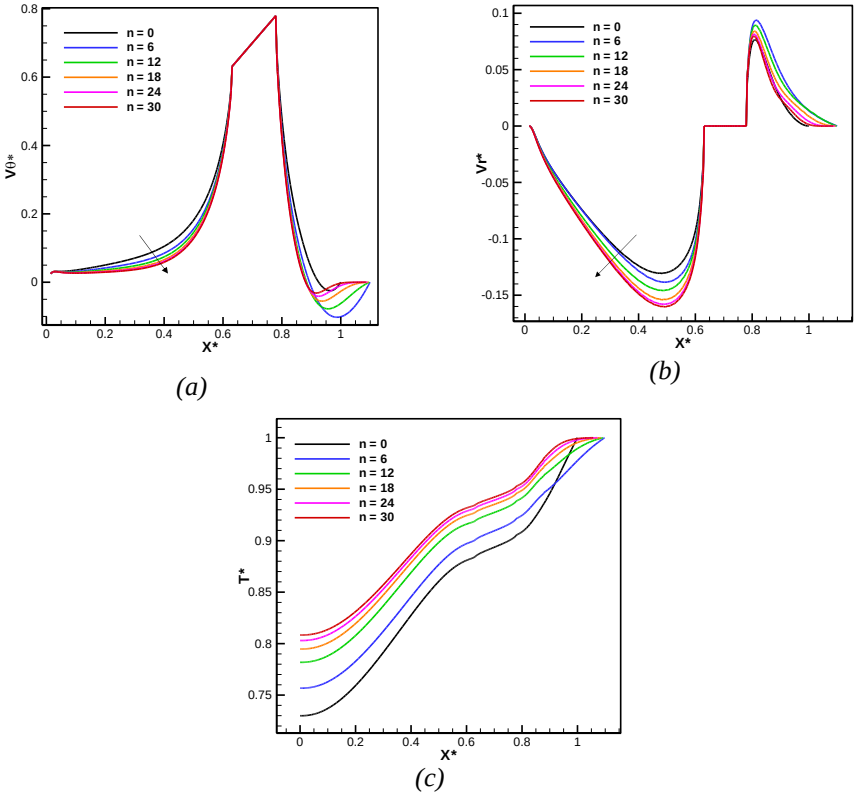

Fig. 5. (a) Tangential velocity (b) radial velocity (c) temperature. At the level of the agitator plane and its extension for different n and for A = 0.1 and φ = 0.04 at τ = 44.

Figure 5 presents the distribution of the tangential velocity, the radial velocity, and the temperature on the line passing through the plane of the anchor and its extension to the wall of the wavy and the standard tank, according to different values of n. The shapes of the velocity curves obtained in this figure are similar to those of the reference [20], except that the presence of undulation on the tank wall means that the tangential component of the velocity decreases significantly between the shaft and the anchor blade 0.05 <X * <0.6, and on the other hand favors an increase in the intensity of the recirculation regions between the anchor blades and the tank wall 0.8 <X* <1.1.

The radial component of the velocity presented in Figure 5 (b) decreases in a similar way as that of the tangential velocity between the anchor shaft and its blades, but between the blade and the neighboring wave, a noticeable jump in the radial velocity has

been recorded from the case of a cylindrical tank (n = 0) to a wavy tank, with n = 6, then a decrease in this velocity was noted with the increase in the wavenumber. This jump can be interpreted by the effect of the amplitude A of the wave, which was set for all the anodes (n = 6 - 30) at 0.1. There is a rapid rise in temperature (Figure 5 (c)) on the line taken from the axis of rotation towards the hot wall in the two cases of a non-wavy wall (n = 0) and wavy wall except the 0.6 <X*<0.8 part corresponding to the blade of the anchor where a decrease in the temperature gradient was recorded given the importance of tangential velocity in this zone and the dominance of forced convection. Moreover, the presence of the waves contributes to very effectively raising the temperature inside the tank. However, the profitability of increasing the temperature decreases with increasing wave number n.

The average Nusselt number is an important overall parameter in heat transfer in stirred vessels. It is considered an indicator of the predominant heat transfer mode in the stirred vessel. Figure 6 shows the evolution of the instantaneous average Nusselt number for a standard tank and tanks with a wavy wall of different numbers n.

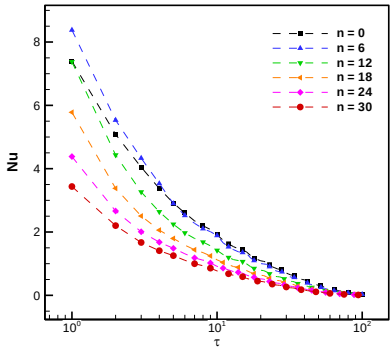

Fig. 6. Instantaneous average Nusselt number for different n for A = 0.1 and φ = 0.04.

The decrease in the average Nusselt number as a function of time indicates the approach to the heat transfer end and the approach to the point of thermal homogeneity inside the stirred tank. This point has been recorded here in the vicinity of the instant τ = 70. We notice that the wavenumber contributes to reducing the average Nusselt number, from n = 6 to n = 30. This indicates that the increasing wavenumber favors the heat transfer mode by conduction and reduces the rate of forced convection. We point out here that this is entirely consistent with the observation we made during our analysis of the streamlines in Figure 4 where we found a large proportion of stagnation within the wave zones, and the stagnation here stimulates the process of heat transfer by conduction. On a special note, it was noticed that there was a jump in the value of the average Nusselt number towards a higher value from the case of a standard tank towards the case of a six-wave. Then, it is indicated that there is a marked rise in the intensity of the forced convection once the waves present in the walls. This does not create an anomaly because the presence of the waves forces the introduction of the wave amplitude. Therefore, the reason for this jump is due to this amplitude which has been fixed here at 0.1 (this corresponds to this that we observed in Figure 4).

The wave amplitude effect

Figure 7 illustrates the effect of increasing wave amplitude on streamlines and isotherms. A decrease in the flow intensity was observed by increasing the wave amplitude. On the other hand, it was observed a widening of the recirculation zone between the blades of the anchor and the vessel wall. Moreover, the temperature increases significantly throughout the tank compared to the standard case.

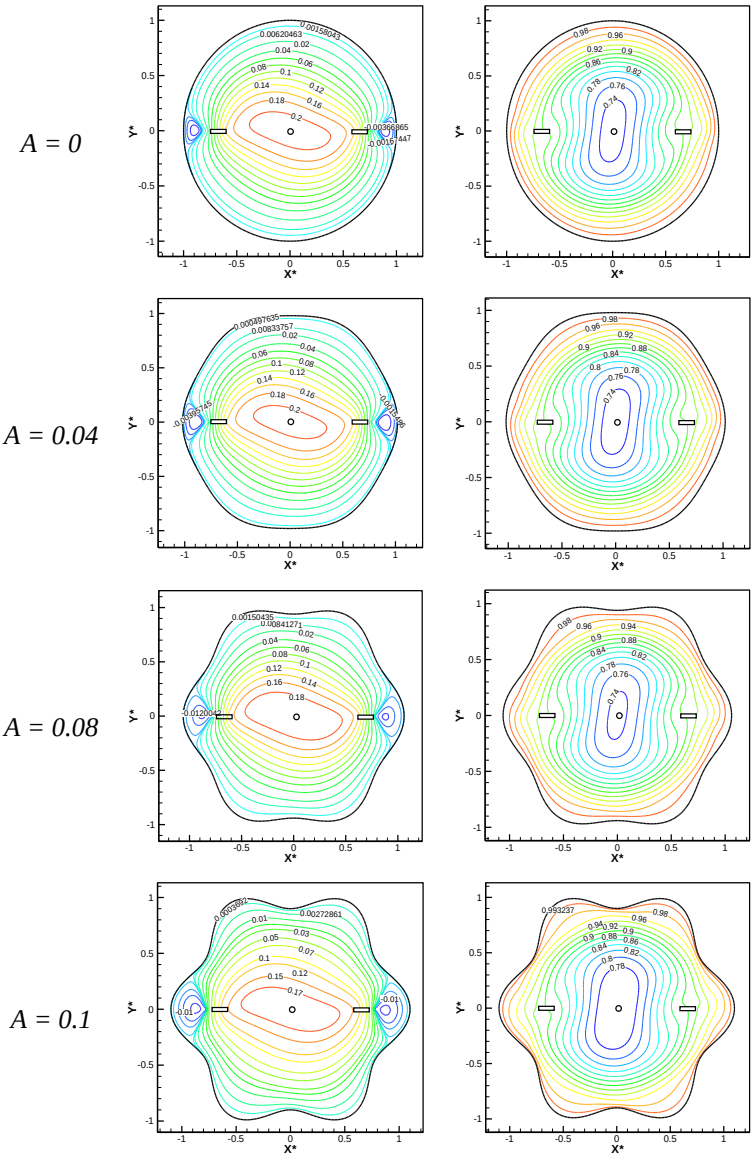

Fig. 7. Streamlines (left column) and isotherms (right column) for different amplitudes with n = 6 and φ = 0.04 at τ = 44.

The variations of tangential velocity, radial velocity, and temperature on the line passing through the plane of the anchor and its extension highlighted by exploring the effect of increasing wave amplitude are respectively presented in Figure 8 (a), 8(b), and 8 (c). The presence of the waves leads to a decrease in the tangential and radial velocities between the shaft of the anchor and its blades (0.05 <X * <0.6). In addition, it leads to an intensifying circular flow between the blades and the wavy wall during the passage of the anchor through this zone 0.8 <X* <1.1 (the negative values of the tangential velocity indicate that the flow is in a direction opposite to that of rotation of the anchor which is translated by the existence of vortices). In the last zone, we see that the amplitude favors the rise of the radial component of the velocity field, which has led to the widening of the vortices observed in Figure 6. In terms of temperature, we see that it increases within the tank with the increase in amplitude. It should be noted that the rate of thermal increase becomes greater for amplitudes of high values.

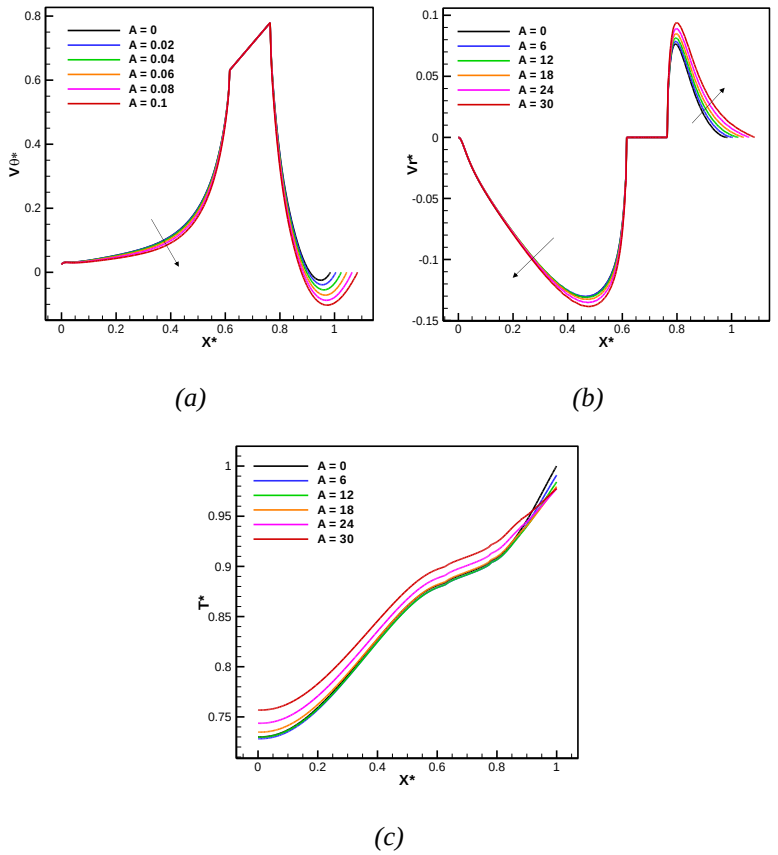

Fig. 8. (a) Tangential velocity (b) radial velocity (c) temperature. At the level of the agitator plane and its extension for different A and for n = 6 and φ = 0.04 at τ = 44.

The instantaneous average Nusselt number presented in Figure 9 indicates that the amplitude has an effect of favoring heat transfer by forced convection due to the rise in the average Nusselt number. It should be noted that the wavenumber of 6 assures us a certain fluidity of the rotary flow by comparing with the high number of waves, and for this reason that the amplitude presented a positive effect on the convective intensity, see Figures 4 and 7.

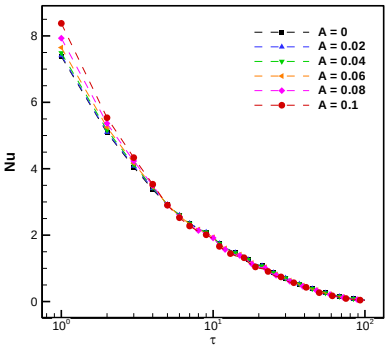

Fig. 9. Instantaneous average Nusselt number for different A and n = 6, φ = 0.04.

The volume fraction effect

The adoption of the technique of adding nanoparticles in the stirred vessel, the wall of which is subjected to a hot temperature, improves heat transfer in the vessel and accelerates the completion of the isothermal state. This is due to the thermal conductivity of solid nanoparticles, which increases the thermal conductivity of the nanofluid. This addition of nanoparticles generally has a low impact on the hydrodynamic behavior due to the very small size of the particles and the low concentrations, which do not exceed 10%.

The examination of the streamlines and isotherms shape in Figure 10, resulting from the change in concentration of alumina nanoparticles inside the water, highlights the effect of these particles on the increase in temperature, which passes at instant 44, from 0.72 to 0.84. On the other hand, no significant change in the stream function is observed. As a result, nanoparticles can maintain the same hydrodynamic trajectory of a nanofluid element with, however, a small change in the intensity of the nanofluid flow.

The investigation of the hydrodynamic phenomenon, in particular tangential and radial velocities, led us to draw the curves of these two components at the level of the line passing through the plane of the anchor and its extension to the tank wall, see Figure 11 (a). The zoom of certain zones of the curves of the tangential and radial velocities showed the impact of the nanoparticles on the variation of these two velocities. Indeed, in the area between the anchor shaft and its blade ($0.02 < X^* < 0.6$), the increase in the nanoparticles concentration up to values close to 0.04, leads to an increase in the tangential velocity of the nanofluid up to a maximum value, then a fall from concentrations greater than 0.04. This same phenomenon is observed for the radial velocity (Figure 11 (b)), the rate of which is opposite (decrease in Vr^* for $0.00 < \varphi < 0.04$ / increase in $Vr^*$for $\varphi > 0.04$). The increase in radial velocity causes the intensity of the nanofluid flow to reduce towards the anchor shaft.

In general, a strong increase in the nanoparticle concentration somewhat leads to a pseudo-reduction in the intensity of the flow while increasing the length of the vortices (recirculation regions), which form between the blades of the anchor and the tank wall.

Figure 11 (c) shows the temperature distribution along the line passing through the plane of the anchor. Regardless of the concentration of nanoparticles, the temperature rises to unity with low-temperature gradients at the anchor blade.

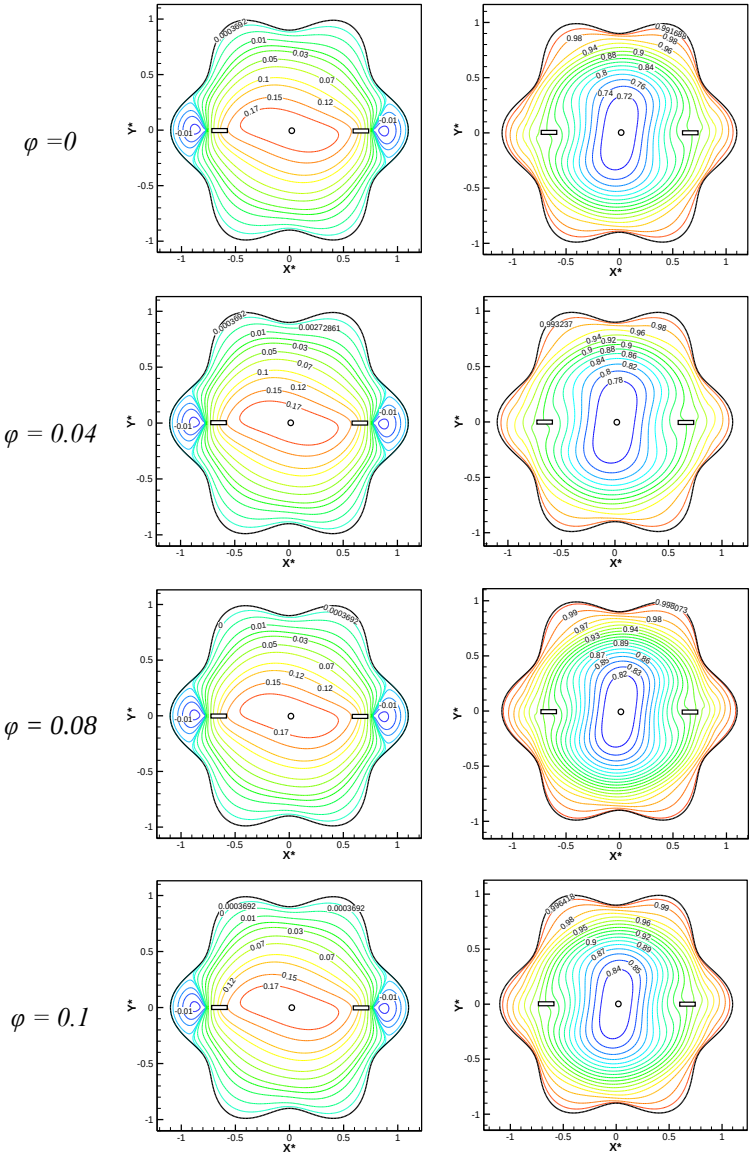

Fig. 10. Streamlines (left column) and isotherms (right column) for different volume fractions with A = 0.1 and n = 6 at τ = 44.

In addition, increasing the concentration significantly increases the temperature (from 0.7 to 0.84) in the immediate vicinity of the anchor axis. This induces an improvement in the heat transfer without observing a significant disturbance in the hydrodynamic behavior inside the tank.

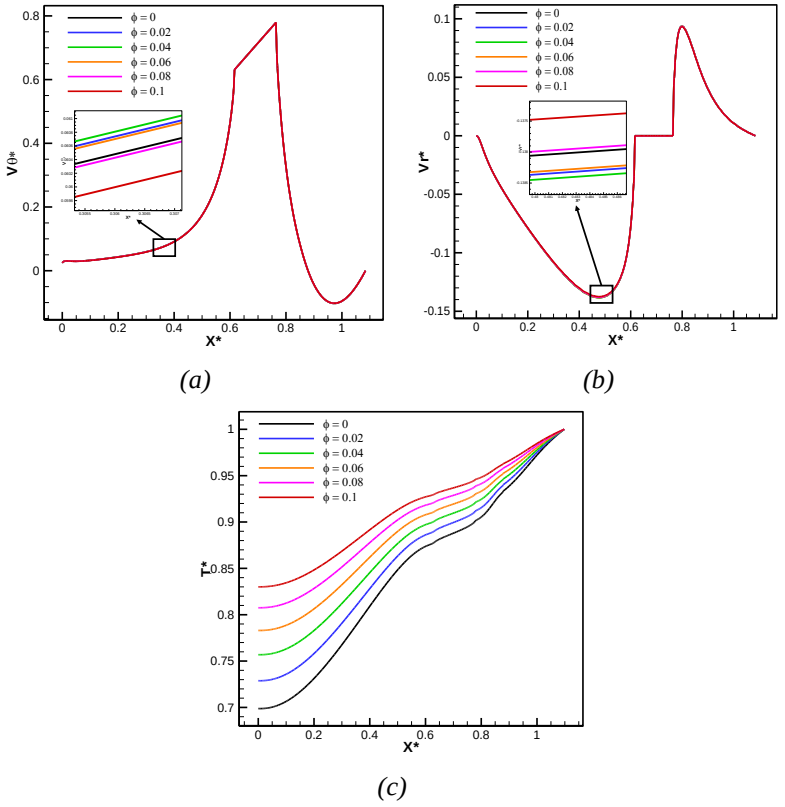

Fig. 11. (a)Tangential velocity (b) radial velocity (c) temperature. At the level of the agitator plane and its extension for different φ and for A = 0.1, n = 6 at τ = 44.

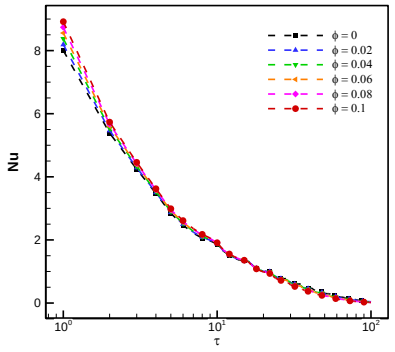

Fig. 12. Instantaneous average Nusselt number for different φ and for A = 0.1, n = 6.

Figure 12 shows the evolution of the instantaneous average Nusselt number as a function of the concentration. We find that the Nusselt number, according to the laws of nanofluids, increases remarkably compared to that of the base fluid (water).

Energy consumption

The inclusion of the contributions from the study of the effect of the addition of nanoparticles and the wavy wall on the thermal level showed remarkable improvements in terms of temperature increase overall of the tank without attempting to increase it by increasing the rate of heating of the wall. It also showed a kind of reduction in the intensity of the flow inside this vessel. In this part, we will discuss the effect of the same factors on the energy consumed during agitation, as it is an inevitable indicator in all studies related to mechanical agitation and mixing operations.

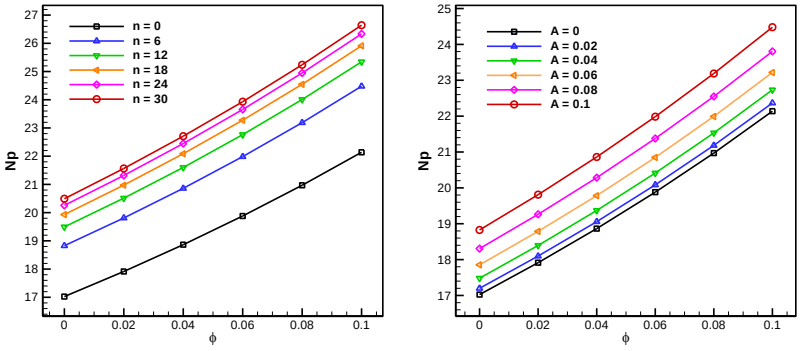

(a) *(b)*

Fig. 13. Power number for different φand (a) different n for A = 0.1. (b) different A for n = 6.

Figures 13 show the evolution of the power number as a function of the concentration of nanoparticles for different wavenumbers (Figure 13 (a)) and different wave amplitude (Figure 13 (b)). The analysis of the two figures shows a significant increase in the power consumed in terms of concentration of nanoparticles, whatever the state of the wall of the vessel (standard state and wavy state from 17 to 22 for $A = 0$). In addition, the power number increases (from Np = 17 to 20.5 for $\varphi = 0$) according to the increase in the number of waves on the one hand and the increase in their amplitude (from Np = 17 to 18.8 for $\varphi = 0$) on the other hand. This recorded increase in terms of nanoparticle concentration is due to the increase in the viscosity of the nanofluid relative to the base fluid. As for the increase in the power number caused by the wave of the tank wall, it is because these waves act as baffles hindering the rotational flow of the nanofluid, which imposes an increase in the quantity of energy supplied to the anchor.

Conclusion

Through this paper, we studied the effect of the wavy wall of a stirred tank equipped with a standard anchor and the addition of alumina nanoparticles in water on the hydrodynamic, thermal, and energy behavior during a laminar flow. The finite element method was used to solve the set of equations governing this phenomenon.

A noticeable improvement in heat transfer inside the tank has been demonstrated as soon as the wall of the tank is wavy, whether by increasing the wavenumber (n = 0 to 36), which favors the process of heat transfer by conduction, by increasing their amplitude (A = 0-0.1) promoting thermal convection, or by introducing nanoparticles of up to 10%. On the other hand, a reduction in the intensity of the laminar flow has been observed due to the baffling role played by the wavy wall during the stirring process and increased fluidity due to the nanoparticles. In terms of energy, a significant increase in the energy supplied to the anchor has been demonstrated in order to achieve the same consumption as it occurs in the standard state and only in the case of the base liquid where we have noted an increase in the power number from 17 (for the standard case) to 20.5 for 6 waves and an increase from 17 to 18.8 for an amplitude of 0.1.

Finally, we conclude that the adoption of the wavy wall technique in order to increase the heat transfer rate in stirred vessels results in excellent heat efficiency, and this also costs in terms of increasing the energy consumed in different proportions depending on the number of waves, their amplitude, as well as the concentration of the nanoparticles.

Nomenclature

Symbols

a	Wave amplitude [m]
A	Dimensionless wave amplitude
Cp	Specific heat [$J.kg^{-1}.K^{-1}$]
d	Anchor diameter [m]
D	Tank mean diameter [m]
da	Shaft diameter [m]
h	Anchor height [m]
H	Tank height[m]
k	Thermal conductivity [$W.m^{-1}.K^{-1}$]
L	Blade length[m]
n	Wave number
N	Rotation speed [s^{-1}]
Np	Power number
Nu	Nusselt number
P	Pressure [Pa]
Pr	Prandtl number
Q_v	Viscous dissipation [s^{-1}]
r	Radial coordinate [m]
R	Tank mean radius [m]
Re	Reynolds number
s	Normal coordinate [m]
t	Time [s]
T	Temperature [K]
U, V	Cartesian velocity component [m/s]
X,Y	Cartesian coordinates [m]
z	Axial coordinate [m]

Greek symbols

φ	Volume fraction
μ	Dynamic viscosity [$kg.m^{-1}.s^{-1}$]
θ	Tangential coordinate [rd]
ρ	Density [$kg.m^{-3}$]
τ	Dimensionless time
ψ	Stream function
*	Dimensionless function

Subscripts

f	Base fluid
nf	Nanofluid
p	Nanoparticles
h, c	Hot, cold

References

[1] R. Metawea, T. Zewail, E. El-Ashtoukhy, I.H. Hamad: Energy, 158 (2018) 111-120.

[2] H. Ameur, M. Bouzit, A. Ghenaim: Journal of Hydrodynamic, 27 (2015) 436-442.

[3] M. Foukrach, M. Bouzit, H. Ameur and Y. Kamla: Chin J Mech Eng, 33 (2020) 33-37.

[4] Y. Kamla, H. Ameur, A. Karas, M. Ilies Arab: Chemical Papers, 74 (2020) 779-785.

[5] M. Major‑Godlewska1, J. Karcz: Chemical Papers, 72 (2018) 1081-1088

[6] S. Woziwodzki, L. Broniarz-Press, M. Ocho-Wiak: J Chemical Engineering and Technology, 33 (2010) 1099-1106.

[7] H. Ameur: Journal of Food Engineering, 233 (2018) 117-125.

[8] H. Ameur: Food and bio products processing, 99 (2016) 71-77.

[9] H. Ameur: Chemical Engineering & Processing: Process Intensification, 154 (2020) 108009.

[10] A. Karas, H. Ameur, R. Mazouzi, Y. Kamla: The International Journal of Advanced Manufacturing Technology,110 (2020) 101–112.

[11] A. Heidari: Chinese Journal of Chemical Engineering, 28 (2020) 2733–2745.

[12] S.U.S. Choi, J. A. Eastman: Developments and Applications of Non-Newtonian Flows, 231 (1995) 99–105.

[13] B.C. Pak, Y.I. Cho: Journal of thermal energy generation, transport, storage, and conversion, 11 (1998) 151-170.

[14] J.A. Eastman, S.R. Phillpot, S.U.S. Choi, P. Keblinski: Rev. Mater. Res, 34 (2004) 219-246.

[15] P. Kamel Chadi, B. Nourredine, G. Belhi, D. Zied: Metallurgical and Materials Engineering 26 (2020) 121-135.

[16] M. Nura Mu'az, C. S.Nor Azwadi, Aminuddin Saat, Bala Abdullahi: CFD Letters, 11 (2019) 104-119.

[17] K. Saliha, A. Mohamed, K. Tayeb: CFD Letters, 11 (2019) 58-75.

[18] J. Bertrand: Agitation des fluids visqueux cas de mobiles à pales, d'ancre et de barrières. Thèse de doctorat, Istitut nationale polytechnique de Toulouse (1983).

[19] M. Baccar, M. Mseddi, M.S. Abid: Int. J. Therm. Sci, 40 (2001) 753–772.

[20] O. Hami, B. Draoui, B. Mebarki, L. Rahmani, M. Bouanini In: Proceedings of cht-08 ICHMT international symposium on advances in computational heat transfer, Marrakech, Morocco, 2008, 10.1615/ICHMT.2008.CHT.1270.

[21] A. Benmoussa, L. Rahmani: Int. Jnl. of Multiphysics, 12 (2018) 209-220.

[22] T. Srinivas, A. Venu Vinod, Experimental Thermal and Fluid Science, 51 (2013) 77-83.

[23] P. Thangavelu, A. Mahizhnan, S. Palani: Chinese Journal of Chemical Engineering, 21 (2013) 1232-1243.

[24] M. Věřišova, M. Dostal, T. Jirout, K. Petera: Chemical Papers, 69 (2015) 690-697.

[25] K. Kamel, R. Mohamed, K. Yacine: Metallurgical and Materials Engineering, 26 (2020) 71-86.

[26] V. Bianco, O. Manca, S. Nardini, K. Vafai: Heat Transfer Enhancement with Nanofluids, International Standard Book Number, Taylor & Francis Group, 2013, 49.

[27] H.C. Brinkman: J. Chem. Phys, 20 (1952) 571–581.

[28] J.C. Maxwell, A Treatise on Electricity and Magnetism, vol. II, Oxford University Press, Cambridge, UK, 1873. p. 54.

[29] S. Nagata, In mixing Principles and applications, (1975) 385-387.
[30] C. Taylor, P. Hood: Comput. Fluids 1 (1973) 73–89.
[31] P. Dechaumphai, Finite Element Method in Engineering, second ed, Chulalongkorn University Press, Bangkok, 1999.